

# Phase-only Synthesis Algorithm for Transmitarrays and Dielectric Lenses

Susana Loredo, Germán León, Omar F. Robledo, and Enrique G. Plaza

Department of Electrical Engineering  
University of Oviedo, Gijón, E33203, Spain  
loredosusana@uniovi.es, gleon@uniovi.es, uo230632@uniovi.es, egplaza@tsc.uniovi.es

**Abstract** — In this work a phase-only synthesis algorithm is applied for the design of lens-array antennas yielding a desired radiation pattern. The potential relevance of spillover effect on the lens radiation pattern is illustrated, making it necessary to include it in the lens model and to take it into account in the synthesis algorithm. Thus, both the contribution of the lens and the spillover radiation are jointly modeled as a planar array. Moreover, in order to validate the algorithm, it has been applied to the synthesis of pixelated dielectric lenses, which have been simulated using a commercial software. Simulations show good agreement with the algorithm results, validating its use for this type of lenses.

**Index Terms** — Antenna array synthesis, dielectric antennas, lens antennas, transmitarrays.

## I. INTRODUCTION

Planar lens-array antennas, also called transmitarrays, consist of a quasi-periodical planar array of printed radiating elements configured to yield a phase distribution that exhibits a collimating effect while ideally transmitting all the incident power [1-4]. Then, in order to achieve a desired radiation pattern, a phase-only synthesis algorithm must be applied to find the necessary phase distribution on the lens surface. Furthermore, the spillover radiation, which propagates in the same region as the radiation from the lens, may affect the antenna behavior. Consequently, the spillover radiation should be calculated and included in the synthesis algorithm and then taken into account to obtain the radiation pattern of the whole system consisting of the lens and the feeding element.

Many different synthesis algorithms have been proposed in the literature, some of them very costly both in time and computational resources. However, the algorithm presented in [5, 6] for the synthesis of low sidelobe radiation patterns is very simple and fast. It is based on the iterative application of direct and inverse fast Fourier transforms, and results are given both for amplitude-only and complex weighted synthesis. In this work that algorithm will be applied to the phase-only synthesis of the radiation pattern of a planar lens-array fed by a horn antenna. The desired pattern will be

specified by two given masks defining the characteristics of both the main lobe and the sidelobe level, so more restrictions are imposed on the algorithm convergence. Moreover, the effect of spillover radiation will be included in the synthesis algorithm.

Finally, in this work it will also be proved that the proposed synthesis algorithm can be applied to the design of dielectric lenses consisting of variable height elements. Dielectric reflectarray and lens antennas have been recently proposed as low-loss, low-cost solutions, based on 3D printing technology, for millimeter-wave and terahertz antennas [7, 8].

## II. PROPOSED APPROACH

### A. System model

The whole antenna system consists of a feeding horn and the planar lens-array, as shown in [9]. The feed is placed at a distance  $F$  from the lens pointing at its center and it is modeled as a  $\cos^q\theta$  function. The lens elements are disposed in a rectangular regular grid made up of  $M_l$  by  $N_l$  elements, as shown in Fig. 1. In this figure, the shadowed area represents the lens, so the dots inside this area represent the lens elements, which are assumed to be isotropic. The field radiated by the feed impinges on these elements, which will modify the incident phase in order to achieve the desired far-field pattern. However, a part of the power radiated by the feed does not impinge on the lens surface since it is radiated at directions beyond the limits of the lens, although it will contribute to the final pattern and will distort it. Then, it is necessary to estimate its effect and include it in the synthesis process. Hence, the incident field from the horn will also be captured in a regular discrete mesh around the lens, represented by the dots outside the shadowed area in Fig. 1. They may be considered as *virtual array elements* following the same regular grid defined for the lens. Therefore the joint effect of the lens-array and the spillover radiation can be modeled as an *equivalent lens-array* of  $M_s \times N_s$  elements, with  $M_s = M_l + 2\Delta M$  and  $N_s = N_l + 2\Delta N$ .

Consequently the array factor (AF) would then be given by:

$$AF(u, v) = \sum_{m=1}^{M_s} \sum_{n=1}^{N_s} I_{mn} e^{j\beta d((m-1)u + (n-1)v)}, \quad (1)$$

where  $I_{mn}$  are the complex excitations at the elements of the *equivalent lens-array*,  $\lambda$  is the wavelength,  $\beta = 2\pi/\lambda$ ,  $d$  is the element spacing,  $u = \sin\theta\cos\phi$ , and  $v = \sin\theta\sin\phi$ , being  $(\theta, \phi)$  the elevation and azimuth angles respectively that define the far-field direction where the AF is being evaluated.

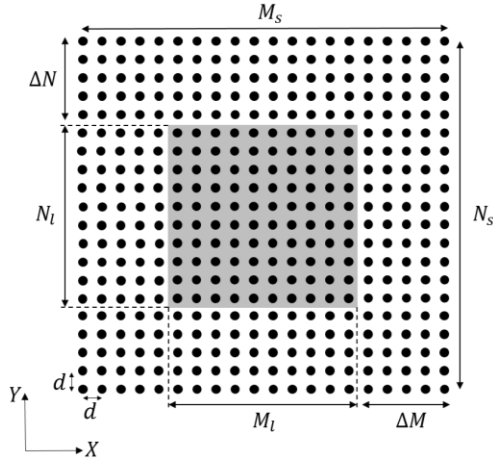


Fig. 1. Scheme of the lens-array model including spillover radiation: *equivalent lens-array*.

This model has been investigated in [9] for transmitarray antennas, comparing it with a Finite Element Method and setting the limits within which it can be used.

## B. Pattern synthesis

The synthesis approach presented in [5, 6] is based on the well-known property that the AF of an antenna array having uniformly spaced elements is the inverse Fourier transform of the array element excitations. Then a direct Fourier transform relationship exists between the element excitations and the AF.

The synthesis procedure starts by defining an initial set of excitations for the array elements. The feed far field, according to the  $\cos^q\theta$  model, will be given by the following expression:

$$\vec{E}_F = j \frac{ke^{-jk r}}{2\pi r} [A_E \hat{\theta} + B_H \hat{\phi}], \quad (2)$$

where

$$A_E = C_E(\theta)\cos\phi, \quad B_H = -C_H(\theta)\sin\phi, \quad (3)$$

for an X-polarized feed, and

$$A_E = C_E(\theta)\sin\phi, \quad B_H = C_H(\theta)\cos\phi, \quad (4)$$

for an Y-polarized feed, with

$$C_E(\theta) = \cos^{qE}(\theta), \quad (5)$$

$$C_H(\theta) = \cos^{qH}(\theta). \quad (6)$$

For an axial symmetric radiation pattern  $qE = qH = q$ . The feed field given by (2) must then be expressed in Cartesian coordinates  $(E_{Fx}, E_{Fy}, E_{Fz})$  and transformed to the lens coordinate system  $(E_{Lx}, E_{Ly}, E_{Lz})$  [10]. As a result, the incident tangential electric field on the lens surface ( $\vec{E}_L$ ) is given by:

$$\begin{pmatrix} E_{Lx} \\ E_{Ly} \end{pmatrix} = \begin{pmatrix} \cos\alpha & \sin\alpha \\ -\sin\alpha & \cos\alpha \end{pmatrix} \cdot \begin{pmatrix} E_{Fx} \\ E_{Fy} \end{pmatrix}, \quad (7)$$

with  $\alpha = 0^\circ$  in case of an X-polarized feed and  $\alpha = 90^\circ$  for Y-polarization. Expression (7) gives the initial value ( $I_0$ ) for the amplitude and phase of the *equivalent lens-array* excitations:

$$(I_0)_{mn} = |\vec{E}_L(x_m, y_n)| e^{j \arg\{\vec{E}_L(x_m, y_n)\}}, \quad (8)$$

being  $(x_m, y_n)$  the coordinates of the element  $(m, n)$ .

For this initial set of the excitations the AF is calculated through a 2-D inverse fast Fourier transform (IFFT) of  $K \times K$  points, with  $K > M_s, N_s$ . The obtained AF is then compared to the masks that define the desired array pattern and those AF values that do not fulfill the specifications are corrected by assigning them a new value into the specified limits.

Applying a 2D fast Fourier transform (FFT) to the corrected AF, the necessary set of element excitations is obtained. It consists of  $K \times K$  samples, of which  $M_s \times N_s$  correspond to the *equivalent lens-array*, so the extra samples are removed. After this, the remaining set of excitations  $(I_1)_{mn}$  consists of:

- 1)  $M_l \times N_l$  samples corresponding to the elements of the lens-array. The amplitude of these excitations is restored to its initial value, since only the phase is allowed to change:

$$|I_1|_{mn} = |I_0|_{mn} \quad (9)$$

$$\text{for } \begin{cases} \Delta M + 1 \leq m \leq \Delta M + M_l \\ \Delta N + 1 \leq n \leq \Delta N + N_l \end{cases}$$

- 2) The samples corresponding to the spillover radiation. They are restored to its initial value, both amplitude and phase, since no synthesis can be applied on the spillover radiation:

$$(I_1)_{mn} = (I_0)_{mn} \quad (10)$$

$$\text{for } \begin{cases} 1 \leq m \leq \Delta M \\ \Delta M + M_l + 1 \leq m \leq M_s \\ 1 \leq n \leq \Delta N \\ \Delta N + N_l + 1 \leq n \leq N_s \end{cases}$$

The IFFT is then applied to this new set of excitations, repeating iteratively the process until specifications are met or the maximum number of iterations is reached.

### C. Effect of spillover radiation

Before applying the proposed algorithm to the synthesis of different patterns, an example will be shown in order to illustrate the effect of the spillover radiation and the convenience of including it into the synthesis algorithm. Let us consider a lens of  $22 \times 22$  elements at the frequency of 16 GHz, being the separation between elements  $d = 0.5\lambda$ . The feed is modeled with  $q = 5$ , and the  $F/D$  ratio is 0.7 (being  $D$  the side length of the lens), resulting in an illumination taper of -10 dB.

The pattern to be synthesized is a flat-top beam one with a ripple of 1 dB and sidelobe level under -18 dB. Initially the synthesis algorithm will not take into account the spillover radiation, that is  $\Delta M = \Delta N = 0$ , and the synthesis will be applied only on the lens-array elements. Then after each iteration a new set of  $M_l \times N_l$  samples are obtained, which are treated as indicated in (2), keeping the synthesized phases and maintaining the initial values for the amplitudes. The pattern obtained with the resulting phase excitations, once the algorithm has converged, is shown in Fig. 2 (*synthesis w/o sp*). It can be observed that it fits into the specifications.

However, in order to prove the relevance of spillover radiation, its effect is added ex-post. After performing the phase synthesis on the lens elements, an *equivalent lens-array* is defined with  $\Delta M = 0.5M_l$ ,  $\Delta N = 0.5N_l$ . The excitations of the elements representing the spillover radiation are given by the feed illumination, whereas the phases of the lens elements are the ones obtained with the synthesis algorithm, which did not have into account the spillover. Fig. 2 shows how the initial pattern (*synthesis w/o sp*) is distorted when the spillover effect is added (*synthesis w/o sp + sp*), showing the existence of side lobes that exceed the limit imposed by the mask. With this system configuration, spillover effects on the far-field pattern should be expected for values of  $\theta$  greater than approximately  $36^\circ$ , since the maximum incidence angle on the lens surface is given by  $\tan^{-1}(0.5D/F)$ . The appearance of these higher level lobes for  $u, v > 0.6$  agrees well with this estimation.

To validate these results a dielectric lens was designed from the phase synthesis results, following a process similar to the one described in [7]. The design of the dielectric lens can be viewed as an array of dielectric slabs with different heights, which will depend on the aperture. Furthermore, in order to minimize the shadowing effects, the elements with maximum height should be placed at the center of the lens. Therefore it may be necessary to add a phase constant to the original phase provided by the synthesis algorithm.

This lens was simulated with FEKO software [11] using Geometrical Optics (GO) approximation. A dielectric lens has been chosen because GO analysis of

the dielectric lens is much faster than full-wave simulation of a transmitarray. Furthermore, dielectric lenses have gained much attention due to their simple manufacture with current 3D printing technology and their potential suitability for mm-wave and terahertz frequencies [7, 8]. The simulation results are also included in Fig. 2 (*GO simulation*), presenting also important side lobes around the mentioned angles. This proves the need of including the spillover effect in the synthesis process.

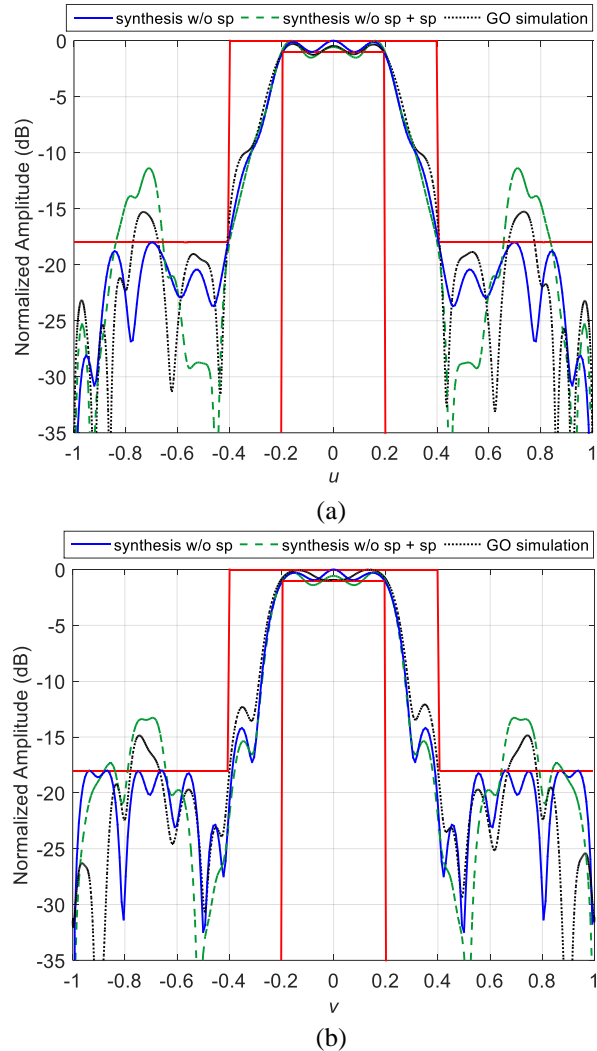


Fig. 2. Effect of spillover radiation. Main cuts for (a)  $v = 0$ , (b)  $u = 0$ .

### III. RESULTS

Once the effect of the spillover in the lens radiation pattern has become evident, the same pattern will be now synthesized taking that effect into account. For that,  $\Delta M$  and  $\Delta N$  have been chosen to be  $0.5M_l$  and  $0.5N_l$  respectively, resulting in  $M_s = N_s = 44$ . In order to set

the value of  $\Delta M$  and  $\Delta N$ , a study was carried out to analyze the effect of varying the size of the plane where the incident field from the feed is captured outside the lens-array. Then, for a given lens-array, the radiation pattern of the *equivalent lens-array* has been obtained for different sizes of the spillover grid. Some variations on the results were observed when increasing the size until reaching an illumination taper of -32 dB on the edge of the *equivalent lens-array*. From there, no significant differences were appreciated when increasing the number of points on the spillover grid. For the example under study, the illumination on borders of the  $44 \times 44$  *equivalent lens-array* is -31 dB relative to the illumination on the center of the lens.

Figure 3 shows the radiation pattern obtained once the algorithm has converged. Direct and inverse FFTs of  $256 \times 256$  points were used and 977 iterations were needed so that all far field directions fulfilled the masks, taking 22.5 seconds in a personal laptop with no special features. The necessary phase distribution on the lens surface is represented in Fig. 4 (a). With this new synthesized phase, after adjusting it as commented in Section II, a new dielectric lens was designed and simulated with FEKO. The resulting lens is depicted in Fig. 4 (b). Since a planar array model is being considered, the phase range of the dielectric lens has been limited to 360 degrees in order to have a quasi-planar lens and ensure the viability of the model. The results of the synthesis model and the simulation of the dielectric lens are compared in Fig. 5. Both patterns are very similar and fit well into the limits given by the masks, proving that the effect of the spillover radiation has been efficiently corrected. Similar results could have been obtained with different lens sizes, even smaller than the analyzed here. Simulations carried out in this study showed that the smallest lens to obtain this pattern should have  $14 \times 14$  elements if  $q = 5$  or  $12 \times 12$  elements for  $q = 10$ . Both the value of  $q$  used in the feed model and the constraints imposed by the desired pattern will impact on the necessary number of array elements and also on the number of iterations needed for convergence.

The proposed algorithm was also applied to the synthesis of an isoflux pattern. In this case, the lens was made up of  $38 \times 38$  unit cells, also with a periodicity of  $0.5\lambda$  at the frequency of 16 GHz, and the feed was modeled with  $q = 10$ . The  $F/D$  ratio was kept at 0.7, and  $\Delta M = \Delta N = 0.5M_l$ , turning out in an illumination taper of -20 dB on the lens-array and -52 dB on the *equivalent lens-array*. Figure 6 shows both the synthesized phase and the dielectric lens designed to validate the model with GO simulation. The 3D pattern obtained with the synthesis algorithm can be seen in Fig. 7. This result required 300 iterations, also with  $K = 256$ , and a computing time of 7.5 seconds. One of the main cuts is compared with the dielectric lens simulation in Fig. 8,

showing a great concordance and good fulfilment of specifications. There is only a small discrepancy between the algorithm and the simulation since the slope of the main beam for the simulated dielectric lens is not as vertical as required between -10 and -15 dB.

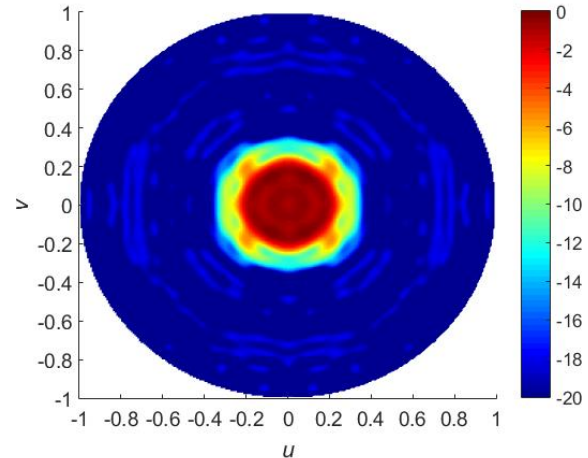


Fig. 3. 3D flat-top beam pattern obtained from phase-only synthesis algorithm.

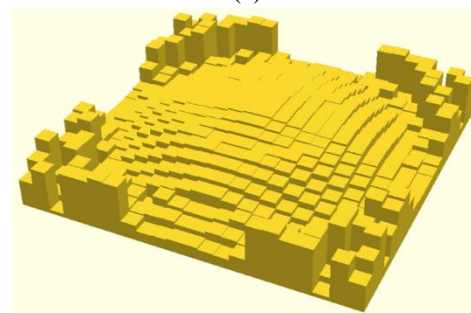
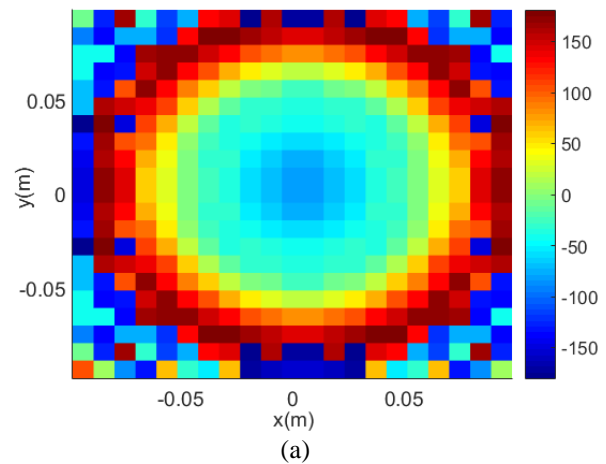


Fig. 4. (a) Synthesized phases, and (b) 3D model of dielectric lens for the flat-top beam pattern.

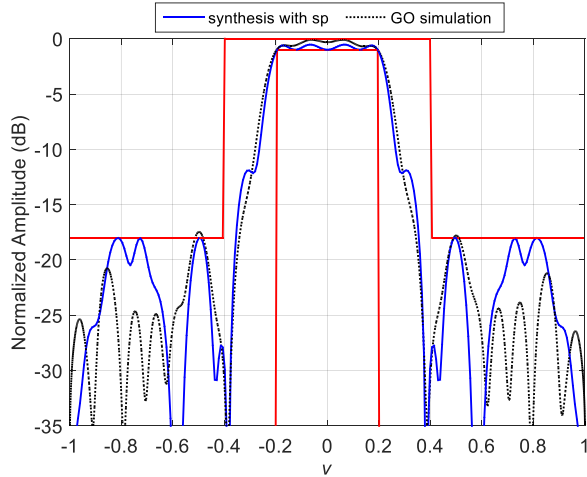
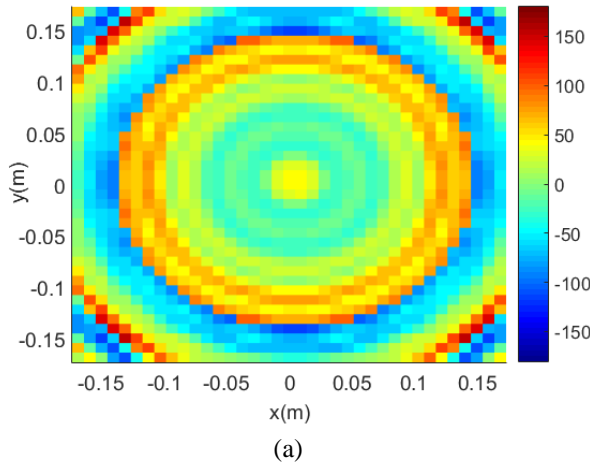
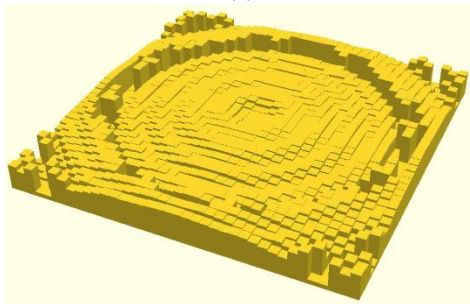


Fig. 5. Cut  $u = 0$  for flat-top beam pattern.



(a)



(b)

Fig. 6. (a) Synthesized phases, and (b) 3D model of dielectric lens for the isoflux pattern.

**IV. CONCLUSION**

A simple and fast phase-only synthesis algorithm has been proposed for the synthesis of lens-array antennas. The algorithm includes the effect of the spillover radiation, modeling the joint effect of the lens-array and the spillover as an *equivalent lens-array*, and

applying iteratively the Fourier transform techniques to obtain the radiation pattern due to both contributions. In order to have the spillover appropriately modelled, the size of the spillover grid must be chosen to produce an illumination taper lower than -30 dB on the edge of the *equivalent lens-array*.

The algorithm is based on a planar aperture model of the lens and is then valid for the design of transmitarray antennas yielding a desired radiation pattern. Furthermore, in this work it has been shown that its use can be extended to the synthesis of pixelated dielectric lenses, made up of square dielectric slabs of variable height, as long as the phase range is limited to 360 degrees so that the lens can be considered quasi-planar. The comparison of algorithm results and GO simulations of dielectric lenses shows both the efficiency of the algorithm to achieve the desired pattern and the good agreement of simulations with the algorithm results. Small discrepancies may be attributed to diffraction and shadowing effects on the dielectric lens.

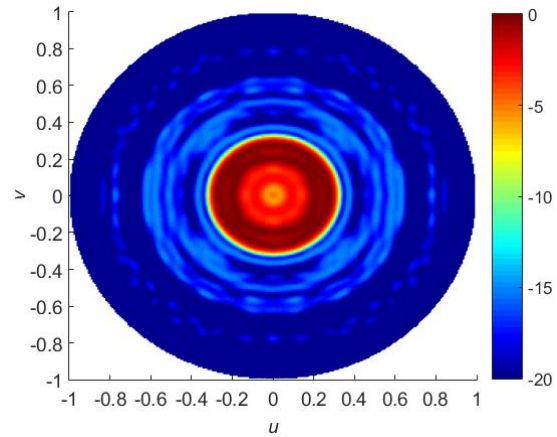


Fig. 7. 3D isoflux pattern obtained from phase-only synthesis algorithm.

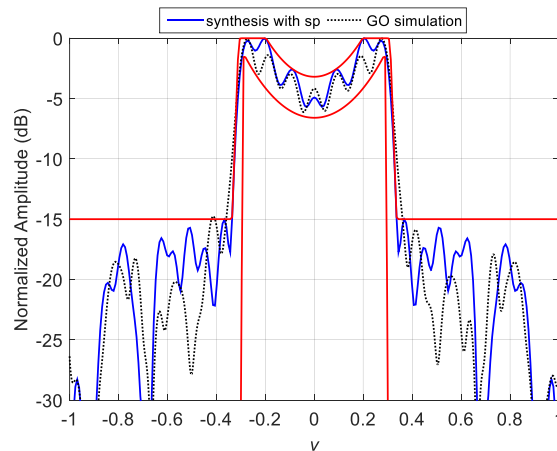


Fig. 8. Cut  $u = 0$  for isoflux pattern.



## ACKNOWLEDGMENT

This work was supported in part by the Ministerio de Economía y Competitividad, under project TEC2017-86619-R (ARTEINE), and by the Gobierno del Principado de Asturias/FEDER under project GRUPIN14-114.

## REFERENCES

- [1] J. Thorton and K.-C. Huang, *Modern Lens Antennas for Communications Engineering*, Wiley-IEEE Press, Hoboken, New Jersey, 2013.
- [2] C. G. M. Ryan, M. R. Chachamir, J. Shaker, J. R. Bray, Y. M. M. Antar, and A. Ittipiboon, "A wideband transmitarray using dual-resonant double square rings," *IEEE Trans Antennas Propagat.*, vol. 58, no. 5, pp. 1486-1493, May 2010.
- [3] S. Zainud-Deen, S. Gaber, H. Malhat, and K. Awadalla, "Single feed dual-polarization dual-band transmitarray for satellite applications," *ACES Journal*, vol. 29, no. 2, pp. 149-156, Feb. 2014.
- [4] L. Di Palma, A. Clemente, L. Dussopt, R. Sauleau, P. Potier, and P. Pouliguen, "Circularly-polarized reconfigurable transmitarray in Ka-band with beam scanning and polarization switching capabilities," *IEEE Trans. Antennas Propagat.*, vol. 65, no. 2, pp. 529-540, Feb. 2017.
- [5] W. P. M. N. Keizer, "Low sidelobe pattern synthesis using iterative Fourier techniques code in MATLAB," *IEEE Antennas Propag. Mag.*, vol. 51, no. 2, pp. 137-150, Apr. 2009.
- [6] W. P. M. N. Keizer, "Fast low-sidelobe synthesis for large planar array antennas utilizing successive fast Fourier transforms of the array factor," *IEEE Trans. Antennas Propagat.*, vol. 55, no. 3, pp. 715-722, Mar. 2007.
- [7] P. Nayeri, M. Liang, R. A. Sabory-García, M. Tuo, F. Yang, M. Gehm, H. Xin, and A. Z. Elsherbeni, "3D printed dielectric reflectarrays: Low-cost high-gain antennas at sub-millimeter waves," *IEEE Trans. Antennas Propagat.*, vol. 62, no. 4, pp. 2000-2008, Apr. 2014.
- [8] H. Yi, S.-W. Qu, K.-B. Ng, C. H. Chan, and X. Bai, "3D printed millimeter-wave and terahertz lenses with fixed and frequency scanned beam," *IEEE Trans. Antennas Propagat.*, vol. 64, no. 2, pp. 442-449, Feb. 2016.
- [9] E. G. Plaza, G. León, S. Loredo, and F. Las-Heras, "A simple model for analyzing transmitarray lenses," *IEEE Antennas Propag. Mag.*, vol. 57, no. 2, pp. 131-144, Apr. 2015.
- [10] Y. Rahmat-Samii, "Useful coordinate transformations for antenna applications," *IEEE Trans. Antennas Propagat.*, vol. AP-27, no. 4, pp. 571-574, July 1971.
- [11] FEKO, ver. 7.0, EM Software & Systems-S.A., Stellenbosch, South Africa, 2014.



**Susana Loredo** received the M.Sc. and Ph.D. degrees in Telecommunication Engineering in 1997 and 2001 respectively, both from University of Cantabria, Spain. In 2001 she joined the Department of Electrical Engineering, University of Oviedo, first as a Research Scientist, and since 2007 as an Associate Professor.

Her research activity in recent years includes radio channel characterization, wireless communications (MIMO systems, vehicular communications), and techniques for echo cancellation and reconstruction of antenna patterns measured in non-anechoic environments. Her interest is now focused on the design of planar lenses and their application to imaging and detection at microwave and millimeter frequencies.



**Germán León** was born in Alcázar de San Juan, Spain. He received the M.Sc. degree and Ph.D. degree in Physical Sciences, from Universidad de Sevilla, Spain, in 1998 and 2005 respectively. In 2005, he joined the Department of Electrical Engineering, Universidad de Oviedo, Gijón, Spain, as an Associate Professor. His research interests are centered on planar lenses, near-field focusing antennas and their applications to imaging and detection.



**Omar F. Robledo** received his B.Sc. degree in Telecommunication Engineering from University of Oviedo, Spain, in 2016 and he is now pursuing his M.Sc. degree. His research activity is focused on synthesis algorithms for planar arrays with application to the design of planar lenses.



**Enrique G. Plaza** was born in Oviedo in 1988. He received his M.Sc. and Ph.D. degrees in Telecommunication Engineering at University of Oviedo in 2012 and 2017 respectively. His main research interests are the design and analysis of planar lenses and their use in imaging and detection applications.